The CASPER mission

Chasing ghosts in the atmosphere

Summer School Alpbach, 21.07.2022

Authors: Lou Byrne, Ulrik Falk-Petersen, Ali A. Hamdoun, Gwendal Hénaff, Kilian Huber, Ilas Andreea Nicoleta, Manuel Maurer, Nadja Reisinger, Jonas Sinjan, Crisel Suarez, András Szilágy-Sándor, Vertti Tarvus, Marialina Tsinidis, Mikhail Vaganov

Tutors: Günter Kargl, Iannis Dandouras

Abstract

CASPER is a two satellite scientific mission operating in Low Earth Orbit (LEO). It aims to answer key questions concerned with Transient Luminous Events (TLEs) and Terrestrial Gamma Ray Flashes (TGFs). Specifically, the mission will constrain the characteristics and origin of such events. Furthermore, their role in the global electric circuit and the coupling between different layers of the atmosphere will be investigated. The mission will be using a train of two spacecraft in a sun-synchronous orbit with an inclination of 98°. The nominal lifetime of the mission is five years, with a possible extension of the mission in respect with the operational status of the instruments. Both satellites will carry the same payload; three low speed, high resolution cameras in various wavelengths as well as four high speed low resolution sensors responsible for triggering the recording of data. Finally, the electron flux from these events will also be measured in order to constrain the role of TLEs and TGFs in the global electric circuit.

1 Background Information

1.1 Introduction

Predicted by C.T.R. Wilson in 1925 [1], Transient Luminous Events (TLE) is a bright, short-lived atmospheric phenomena, which was captured for the first time in 1989. Since then, many different types have been identified. Previous surveys suggest that there is a connection between thunderstorms and TLEs, however, the exact mechanisms are not yet clear, as the data retrieved from previous missions (ground, aircraft, balloon and ISS) had spatial, temporal and measurement limitations.

Another related phenomenon, Terrestrial Gamma Ray Flashes (TGFs) are also linked to TLEs and thunderstorms. With the discovery of these events several theories emerged to explain the formation mechanism and their role in the global energy balance. Moreover, their impact is believed to include [2]:

● Spontaneous transfers of energy from Troposphere to the Ionosphere
● A role in the chemical balance in the upper atmosphere
● Contribution to the perturbation of the population in radiation belts
● New plasma physics mechanisms

1.2 Scientific Background

Transient Luminous Events (TLEs) have a typical lifespan of 0.5 ms to 5.0 ms, however, they vary greatly depending on the specific type of TLE. The events can reach up to 500 km in width, though most are smaller than 200 km [3,4,5]. The phenomena appears in altitudes between 20 and 100 km above ground and are more common in latitudes ranging from -65° to 65° which can be seen in Figure 1. [6,7]. There is one main theory concerning the formation mechanism of TLEs, called the Quasi-Electrostatic (QE) Model. Due to conventional cloud-to-ground (CG) discharges during thunderstorms, a rapid change in charge distribution occurs, creating a quasi-electrostatic field which is 2-3 times stronger than the conventional breakdown field. [8,9]. Random

triggering events can then cause TLEs, these may include CG-lightning, Cosmic Rays and precipitated electrons from the Van Allen Belt and micrometeors [3,10,11,12]. The triggers increase the electric field, which causes upward propagating electrons, ambient heating and ionization in the upper atmosphere and thus emissions. However, this model cannot explain certain characteristics of TLEs, such as occasionally observed spatial and temporal disconnections from the thunderstorm. [13,14]. Furthermore, different types of TLEs exhibit different behaviors, Elves, for example, occur primarily above oceans, while sprites occur more often above land. [15].

Terrestrial Gamma Ray Flashes (TGFs) are intense gamma ray emissions with an extremely short lifetime of 10µs to 100µs . The mechanism is similar to that for TLEs, however, the accepted theory proposes that electrons are accelerated to relativistic energies in a runaway avalanche effect [16]. The Fermi mission measured single photon energies of up to 40 MeV. [17,18]. They have been observed to be correlated with lightning. [19,20].
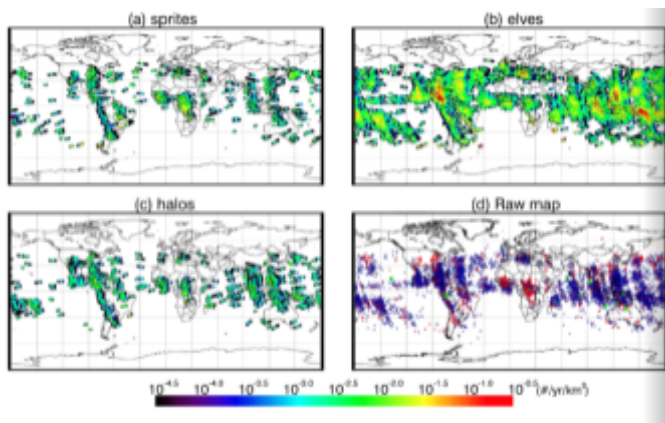
Figure 1: Global Distribution of TLEs using data gained from ISUAL [6].

1.3 Comparative Aspect

Theoretical work has predicted that TLEs should be present on other planets [21]. In fact, the Juno mission observed 11 bright flashes with an average duration of 1.4ms at 260km altitude above Jupiter's 1-bar-level. The measured events have characteristics comparable to TLEs on Earth. [22]. Additional understanding of TLEs and TGFs on Earth will inform us of the interaction between the atmospheres of other planets and their magnetized environments.

2. Science Case

2.1 Scientific Objectives

The goal of the mission is to study upper atmospheric discharges to gain understanding of their origin and their role in the interaction between atmosphere, ionosphere and magnetosphere. These are expressed in the following science objectives (SO) with sub-science objectives (SSO):

SO-1: Constrain the mechanism by which TLEs and TGFs originate and their link

SSO-1: Characterize the spatial and temporal connection between thunderstorms, TGFs and TLEs
.
SO-2: Constrain the extent to which TLEs and TGFs play a role in the interaction between the Atmosphere, Ionosphere and Magnetosphere

SSO-2: Quantify the energy transfer to the upper atmosphere and space

SO-3: Identify the influence of environmental conditions

SSO-3: Measure data over a spectrum of different environmental conditions, including but not limited to: solar cycle, sea surface temperature, geographic position, global distribution.

2.2 Scientific Requirements

The following scientific requirements have been designed to satisfy the aforementioned scientific objectives.
SR-1: Global Mapping of TLEs and TGFs
SR-2: Spatially resolve TLEs horizontally and vertically
SR-3: Temporally resolve TLEs and TGFs

SR-4: Measure energy spectrum of the TLEs and TGFs

SR-5: Detect electron flux from TLEs and TGFs

SR-6: Discriminate downward from upward electron fluxes

SR-7: Identify lightning events

2.3 Measurement Requirements

The measurement requirements translate the scientific requirements into tangible instructions, which can be used to help answer these requirements.

MR-1: Vertical Structure

MR-2: Minimum Spatial Resolution of 0.5 km (horizontal & vertical)

MR-3: Minimum Temporal Resolution of 0.3 ms

MR-4: Observational wavelengths required: (762 nm, 777 nm, 150-280 nm, Gamma Ray to 10 MeV, X-Rays from 20 keV)

MR-5: Upwards Propagating Electrons (10 keV-40 MeV)

MR-6: Downwards propagating electrons (30 keV-300 keV

Key reasoning regarding MR-4, MR-5 and MR-6

One of the most prevalent wavelengths of TLEs (762.7 nm) lies near the O_2 absorption line of 761.9 nm. Therefore a considerable amount of lightning will be absorbed by the atmosphere.

To further discriminate between lightning and TLEs, we introduce a three high-resolution camera system.

● The first two are centered on 777 nm for lightning detection, 762 nm for TLEs and TGFs detection. The same system was proposed for the TARANIS mission [30] and has successfully been employed by the LSO (Lightning and Sprite Observations) experiment on the ISS [2].

● The third camera will be centered on a Far UV band to observe the LBH (Lyman-Birge-Hopfield) emission band of

Nitrogen. Previous studies have suggested that this band is not contaminated by lightning due to absorption, while still being one of the strongest emission lines of TLEs. [7]

MR-5 and MR-6 will be used to discriminate downward- from upward propagating electrons to determine their origin. Previous studies suggest electrons originating from TLEs and TGFs to have energies of 10 keV to 10 MeV and electrons precipitating from the Van Allen Belt have energies of 30 keV to 300 keV. [23] (upper limit), [24] (lower limit), [25], [26] (both Van Allen Belt).

From the ISUAL global survey [6], global detection rates per min for different types of TLEs were calculated. With our desired field of view of 512x512km on the Tropopause and mission profile, 0.09 % of the area where TLEs and TGFs are known to detect, will be covered by our spacecraft per minute when our instruments are operating. Extrapolated to our total mission orbit, this results in approximately 2500 TLEs. Finally the TGFs detected per day are from the ASIM mission. The mission detected 0.7 TGFs per day, taking our more inclined orbit into account, we estimate 0.5 TGFs per day [31]. Since Gigantic Jets are the rarest type, to detect at least 20 such events, an operating time of at least 4 years is required. These estimations are conservative estimates, as empirical data from ISUAL implies to expect an average of 10 Gigantic Jets per year.

Table 1: Expected Detected Events

Type	Raw occurrence / min	Detection / Mission year
Elves	3.62	~1800
Halos	0.37	~180
Sprites	0.42	230
Gigantic Jets	0.01	5
	Detection Rate /day	Detection Mission / year
TGFs	0.5	~180

3. Instruments and Mission Concept

3.1 Mission profile

We aim to observe TLEs and TGFs with a high spatial and temporal resolution (MR2, MR3) and on several wavelengths for photons (MR4) and energy ranges for electrons (MR5, MR6). Additionally, we aim to observe the vertical structure of these events (MR1). We therefore introduce a mission profile composed of two spacecraft on a train with identical payloads in order to resolve the vertical structure of these phenomenons, as shown in Figure 2.
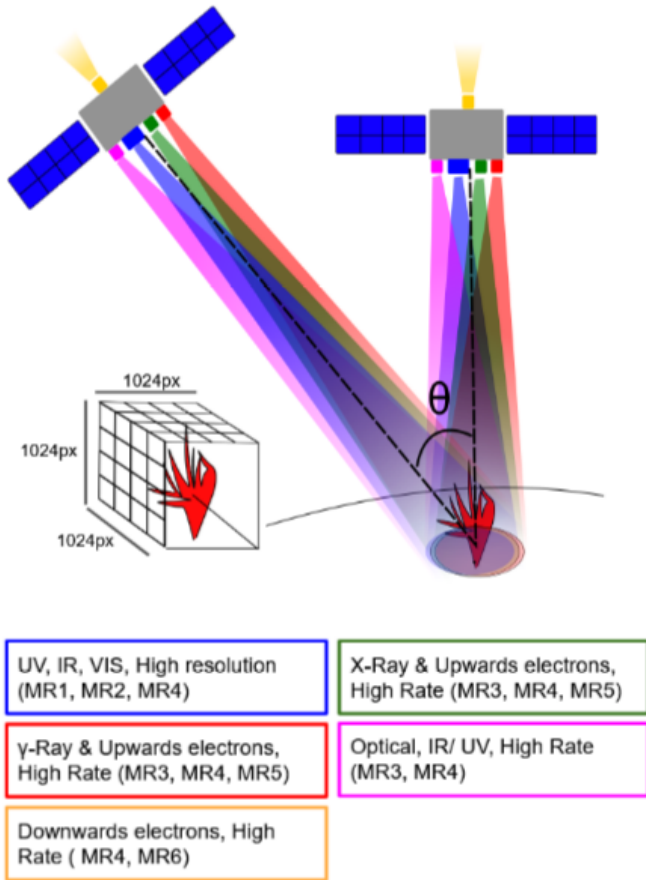
Figure 2: Observation concept of the mission

The onboard instrumentation, when combined, will answer all measurement requirements. Due to the technical impossibility to make observations at high speed, high resolution and several wavelengths with the same technology, separate instruments will be used, as shown in Figure 2.

The UV, IR, Visible observations will be done at high resolution. The spacecraft separation distance, and therefore the angle Θ, is the key parameter to control the vertical resolution of the TLEs and TGFs. This has been estimated to be 42.5° as a compromise between the distance from the region of interest, reduction of projection effects and vertical resolution.

All instruments will observe the same area with different temporal and spatial resolutions. Based on early calculations, a nominal field of view is of 40° for the spacecraft pointing nadir and of 12° for the spacecraft on limb.

3.2 Instrumentation choice

The payload is selected to fulfill the mission requirements mentioned in section 2.4 and 3.1. All instruments are rated TRL 6 or above. The following instruments in table 2 will be operated on each spacecraft:

Table 2: Operating instruments

Instrument	Observed parameters	Spatial resolution	Rate	TRL
IPVIS (x1)	740-780 nm	1 px	300 Hz	TRL 8
IPG (x1)	γ-ray	1px	300 Hz	TRL 8
IPXI (x1)	X-ray	1px	300Hz	TRL 8
ROTCAM (x3)	UV IR 740-780 nm	1024*1024 px	60 Hz	TRL 6
DELEC (x1)	10MeV electrons	1 px	300Hz	TRL 8

3.3 Instrumentation operation

We aim to observe events at high speed and high rate following the requirements in section 2.4. We introduce the concept of trigger instruments (UPVIS, IPG and IPXI), as shown in Figure 3. Trigger instruments will have their data continuously saved on the flight computer's hard memory. The ROTCAM systems will continuously operate and record data on a shift register based on a first in last out basis, meaning that it will be filled with the most recent images. ROTCAM data will be written to the hard memory when trigger instruments detect an event. The shift register size will be set so that extended TLEs and TGFs can be properly recorded.
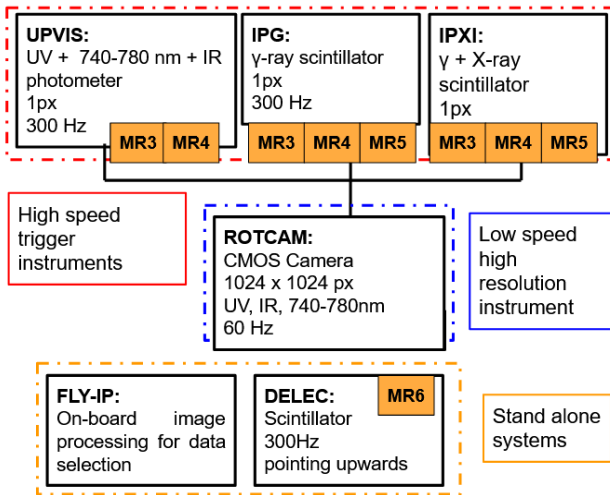
Figure 3: On board instrumentation.

3.4 Instrumentation details

ROTCAM is a low-speed, high resolution instrument composed of three off-the-shelf Teledyne CMOS Cameras able to operate different wavelengths (193-400 nm, 400-700 nm and 700-1000 nm), with a frame rate of 60 Hz and a resolution of 1280x1024 px. Resolution will be reduced by masking pixels to have an image size of 1024x1024px.

IPG, IPXI and DELEC are sensors in a sandwich configuration made of two BC-408 plastic scintillators enclosing a $LaBr_3$ crystal scintillator and running off a high voltage power supply. Operating at 300 Hz, they will only record the intensity on one pixel with a field of view of 40° for the spacecraft pointing nadir and 12° at limb. $LaBr_3$ scintillators have a response centered on 62 keV and 332 keV [27], therefore allowing detection of γ-ray and X-ray. Relativistic electrons can be detected by the stacked plastic layers below the $LaBr_3$ crystal. as required by MR-5 and MR-6. DELEC will be pointing upwards to follow MR-6. IPG will operate with an X-Ray shield to detect only γ-ray photons and relativistic electrons. IPXI will detect both γ-ray and X-ray photons plus relativistic electrons. Using IPG and IPXI simultaneously allows to get the photon count on both the γ-ray and X-ray bands plus electrons between 10 keV to 40 MeV, therefore following MR-4 and MR-5.

UPVIS is an optical photometer operating at high voltage. It is pointed downwards measuring UV, IR and 750-780 nm at 300 Hz. It has a field of view of 40° at nadir and 12° at limb.

3.2 Mission Concept

The mission requires both high spatial and temporal resolution, which are mutually exclusive. Thus, the instruments will be cooperating to gain information both in temporal and spatial distribution. All instruments will be operating continuously and writing data onto a circular buffer on a first-in-last-out basis. UPVIS, IPG and IPXI are designed to trigger at a given intensity threshold, which will be set by scientists, sending a signal to ROTCAM to save the images from the buffer to hard memory.

Furthermore, the two satellites are able to communicate and have synchronized timekeeping using GPS. If it should occur that only one satellite detects an event, it will send a signal including the time stamp to the other satellite, triggering the saving of data. The line-of-sight between the two spacecraft will be 640km: a light travel time of 2ms, with extra processing steps by the sender and receiver, the communication time will be on the order of 5 ms. With a buffer size of 1s, regardless of which spacecraft sends the trigger signal, the desired frames of interest will be in the buffer memory and thus can be written to physical memory.

3.3 Data Processing

On average we expect 15 events/day, from past studies it is known that there are roughly 100 lightning events per TLE/TGF. Lightning only events will be discarded automatically as they will only trigger UPVIS at 777 nm. However we still expect false events that trigger several photometers. We conservatively estimate 150 false events. As each frame is 3 MB and 30 frames/event are required for each of the 6 cameras, the expected data volume is 90 GB/day. While this is possible to downlink to ground with X-band technology, on board data reduction will be utilized as a redundancy, in case of unexpected loss or reduced ground communication, allowing

for scientific operations to continue while downlink is restored.

3.4 Mission Overview
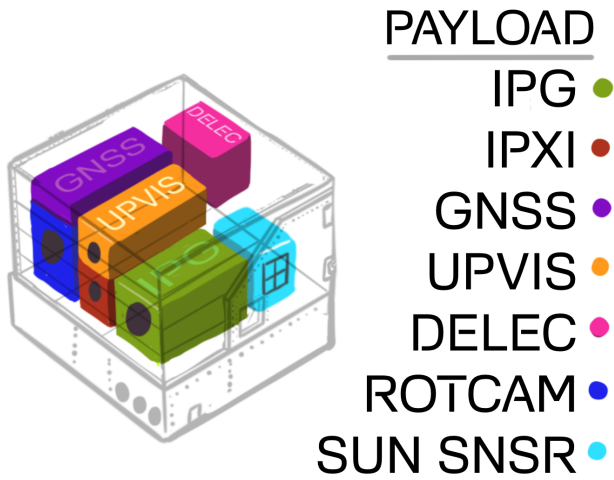
Figure 4: Payload placement on the spacecraft.

The mission is proposed as an F-Class mission with respect to ESA standards. The nominal mission lifetime will be 5 years in a sun-synchronous polar orbit.

4. Space Segment

4.1 Orbit Selection

In order to meet the requirements mapped out in Section 2, the mission will employ a train of two identical spacecraft, orbiting at an altitude of 670 km with an inclination of 98°. While most observations are expected around the equator, the need for a polar orbit arises from MR-5, and the fact that the electrons follow the magnetic field lines. This results in 70 min of observation time per orbit between +65° and -65° of latitude. Moreover, a sun synchronous orbit has been chosen to have constant lighting conditions between successive observations. The orbit height is limited minimally by atmospheric drag at 500 km and maximally at 800 km by excessive background radiation. An altitude of 670 km has been chosen to strike a balance between maximizing both ground coverage and resolution.

The chosen orbit will have a Right ascension of ascending note (RAAN) rate of 9.5°/day with 14 passes/day. This implies a period of 96 min and an ascending node time of 10:30am. To achieve this orbit, the spacecraft require a ΔV of 75 m/s for phase maneuvers, 70 m/s to deorbit and a margin of 10 m/s for a total of 155.5 m/s.

SR-2 dictates the necessity for vertical resolution of TLEs, the satellites will thus be flown in a train formation, with a set phase angle, such that the fields of view overlap in the area of interest. Since the viewing angle between spacecraft is estimated to be 42.5°, this corresponds to a phase angle of 5.2°. This gives the mission the capability of performing stereo imaging of TLEs. To ensure that MR-2 is fulfilled, the required pointing accuracy is <1°. The coverage achieved with this setup is 50 % of the surface in one day, 80 % in two days and 96.5 % in seven days.

4.2 Launch

With the low mass of the spacecraft and the common orbit, it is possible to use a rideshare mission to launch the satellites into orbit. This reduces costs and ensures that both satellites are placed in identical orbits before initiating the plane change. If needed, the mission can also be launched on a dedicated launcher that can accommodate the two spacecraft at the same time, such as the Vega rocket.

Considering the growth of the New Space segment in Europe, there is a possibility that microlaunchers can support frequent launches in a few years' time. Companies such as Isar and RFA are on track to launch their first rockets from Andøya in Norway next year, and have a payload capacity of 1000 kg. [28, 29] These vehicles can bring both satellites to orbit on a single launch, at a very low cost.
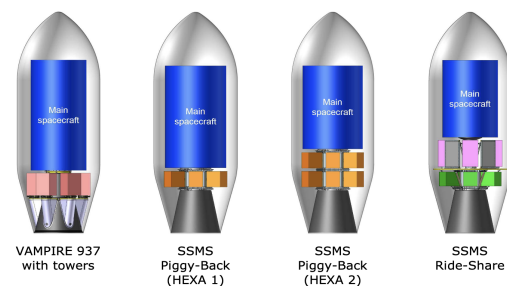
4.3 System and Science Risks

The two satellites of the Casper mission are planned to operate at Low Earth Orbit with an off-the-shelf instrument package rated at TRL 6 or higher. This means the only specific mission risks consist of the ability to get the FPGA and CMOS camera space qualified in time. Since the science mission does not depend on a narrow launch window the consequences would be increased development cost of the camera system. Aside from this, any other risks are standard risks for LEO missions. That includes launch failure and system or component damage due to collision with space debris.

4.4 Operation modes

The mission will have four different Operational Modes depending on the geographic position.

Mode 1 (Standby): Data Processing phase, the scientific instruments will be turned off.

Mode 2 (Reduced Operations): Day Pass, the scintillators and the photometers will be collecting data, the camera will be in standby-mode.

Mode 3 (Data Link): Reserved for Rx and Tx Data Transmission to Esrange. The scientific instruments will be turned off.

Mode 4 (Full Operations): During night pass, all scientific instruments will be recording data.

5. Spacecraft Design & Instrument Integration
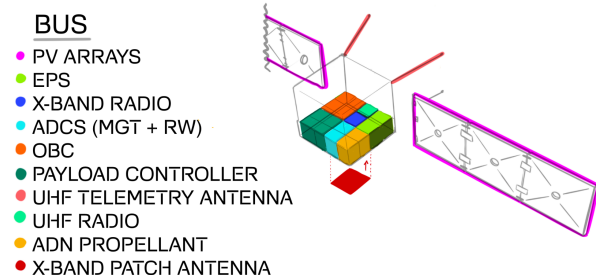
Figure 6: Packaging of instruments inside MP42

Two options for a spacecraft bus were considered. The first was to follow ESA convention and develop a proprietary spacecraft bus with an integration partner as has been done on most ESA missions to date. The second was to investigate the use of an off-the-shelf bus that meets our system requirements and has sufficient flight heritage. A number of bus providers were considered, including Reorbit's Gluon bus that conforms to most system requirements but lacks a sufficient solar array configuration to meet the power requirements. The NanoAvionics MP42 is a flight-proven bus that meets all of our system requirements, with > 20% system margins for every requirement. The bus has the following specifications:
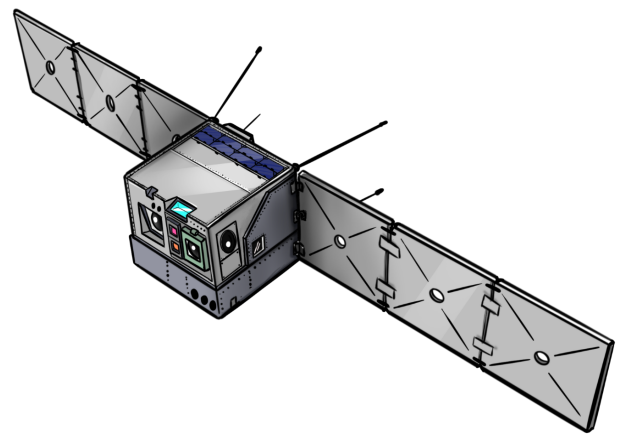
Figure 7: NanoAvionics MP42 bus specified to meet mission requirements.

- TLR 9
- Volume: 500 x 500 x 700 mm
- X-band TX: 500 Mb/s
- Solar Arrays: 237 W
- Bus mass: 45 kg
- Monoprop thruster: 1N
- Magnetorquer + 4 Reaction wheels.
- ΔV: 170 m/s

5.1. Thermal Control

The thermal control ensures that no on-board satellite exceeds the operational limits. Due to the individual operation modes, there are two different cases for the thermal control system: burst mode for the hot case with a power dissipation of 30 W and a standby mode for the

cold case with 8.5 W. The different heat sources for both cases are visible in Table 2. The satellite bus is configurable with a 50 W radiator. Furthermore there are heaters for critical components: battery pack, EPS and propulsion system.

Table 3: Thermal control system for two cases:

Heat source	Hot Case	Cold Case
Electronics (W)	30	8.5
IR earth (W/m^2)	258	216
Albedo (W/m^2)	466.62	0
Sun (W/m^2)	1368	0

5.2. Budgets

5.2.1 Power

Considering all spacecraft subsystems and a 20% margin, the power draw is 121 W in burst mode, the most power-intensive mode of operation. The details can be seen in Table 2.

Table 4: Power Budget

Subsystem	Margin	Mode 1: Standby (W)	Mode 2: Day Pass (W)	Mode 3: Downlink (W)	Mode 4: Night Pass (W)	Mode 4.1: Burst (W)
Payload	10%	-	28	-	5	28
Thermal Control	5%	10	10	10	10	10
C&DH	5%	5	5	5	5	5
Communication	5%	2	2	8	2	2
ADCS	5%	-	30.5	30.5	30.5	30.5
Propulsion	5%	-	-	-	8	-
Other	5%	-	-	-	-	25
Subtotal		17	45	54	61	101
Margin		20%	20%	20%	20%	20%
Total		20	54	64	73	121

To accommodate these needs, a battery of 300 Wh has been chosen in combination with a 238 W solar array. The battery will be able to charge for 48 min/orbit, equaling 146Wh of charge per orbit. For the battery, a Beginning of Life (BOL) efficiency of 30% and an End of Life (EOL) efficiency of 16% has been assumed which has been taken into account when choosing the battery size.

5.2.2 Communications Budget

The chosen ground station is Esrange, in Kiruna, Sweden. The high Latitude maximizes access time. The chosen orbit will have 12 passes/24 hrs for a total of 8000 seconds of access per 24 hrs. Using the X-band downlink with a data rate of 500 Mb/s, the satellites require 1500 seconds of access per day, which equates to 19% of the total available access time. Additionally, the mission will require 300 TB of ground storage.

5.2.3 Mass Budget

The budget for the total payload mass is 35 kg and considering spacecraft mass, the total wet mass is 146 kg. The initial dry mass estimate was calculated as a ~3x multiple of the payload mass for this size of mission. The remaining subsystems were calculated based on a sizing guide from SMAD Space mission engineering book by Hawthorne, CA, Microcosm Press.

Table 5: Mass Budget

Spacecraft Mass				
Subsystem	% of Dry mass	Mass (Kg)	% Margin	Mass+ margin (Kg)
Payload	31%	35	0%	35
Structure	27%	30	5%	32
Thermal Control	2%	2	5%	2
Power (inc. S/A)	21%	24	5%	25
Communications	2%	2	5%	2
On Board Computer	5%	6	5%	6
Attitude Control	6%	7	5%	7
Propulsion	3%	3	5%	4
Other	3%	3	5%	4
Dry Mass	100%	112	-	116
System Margin	20%	23	-	139
Propellant	2%	6	20%	7
Total Wet Mass	-	141	-	146

5.2.4 Cost Budget

Similar to the mass budget, the SMAD book was used to scope the cost of the mission. The mission segment, from design to launch is 38 million euro. The largest cost in operating the spacecraft is the

scientific operations as up to 300 TB of data will need to be analyzed by a scientist. The use of a rideshare with the Vega rocket will cut launch costs to close to ¼ that of a regular launch per spacecraft. This brings the total cost of the mission to 143 million euro over its entire lifespan.

Table 6: Cost Budget

	1x Spacecraft	2x Spacecraft
Spacecraft elements	**Million €**	**Million €**
Structure	1.5	3
Thermal Control	0.9	1.8
ADCS	1.2	2.4
Electrical power supply	2	4
Propulsion (reaction control)	0.8	1.6
Telemetry Tracking and Command	1	2
Command and data handling	1.2	2.4
Payload	2	4
Installation assembly and test	2	4
Engineering, software	10	12
Mission Segment SubTotal	**23**	**38**
Program management	10	10
Mission operation	10	10
Science operation	12	12
Data Storage	0.6	0.6
Industrial cost	15	30
Shared Launch	10	20
Initial cost	**80**	**120**
Margin	20%	20%
Total cost	**96**	**143**

6. Descoping Options

Two Descoping options are proposed. Firstly, the three CMOS cameras could be combined into one using a filter wheel. This would lead to the loss of spectral comparison data, as only one filter can be applied at any given time. The main scientific objectives could nevertheless be fulfilled. Secondly, the mission could be restructured to one spacecraft. While the modified version would still be viable and produce new data, the main scientific goal of simultaneous vertical and horizontal resolution would be lost.

7. Conclusion

The first recorded observation of this plasma phenomenon (TLE) was in 1989.
By implementing CASPER, a two satellite train, we can further the understanding of the mechanism called TLEs and TGFs as well as their link to thunderstorms. The relationship between the Earth's atmosphere and space is critical to understand the energy exchange through the atmosphere. Furthermore, various influences of other environmental factors on the formation of TLEs and TGFs can be examined, such as solar cycles, geographic position, sea surface temperature and global mapping.

8. Bibliography

1. Wilson, C. T. R. (1925), The electric field of a thundercloud and some of its effects,Proc. Phys. Soc. London,37, 32D–37D.
2. Blanc et al. (2007), A microsatellite project dedicated to the study of impulsive transfers of energy between the Earth atmosphere, the ionosphere, and the magnetosphere. Adv. Space Res. 40, 1268.
3. Wescott, E. et al. (2001), Triangulation of sprites, associated halos and their possible relation to causative lightning and micrometeors, J. Geophys. Res., 106(A6), 10467– 10477
4. Marshall, R. et al. (2006). High-speed measurements of small-scale features in sprites: Sizes and lifetimes. Radio Science, 41(6), RS6S43.
5. Kuo, C.,et al. (2013). Ionization emissions associated with N_2^+ 1N band in halos without visible sprite streamers. Journal of Geophysical Research (Space Physics), 118(8), 5317-5326.
6. Chen, A. et al. (2008). Global distributions and occurrence rates of transient luminous events. Journal of Geophysical Research (Space Physics), 113(A8), A08306.
7. Blanc, E. (2010). Space observations of Transient Luminous Events and associated emissions in the upper atmosphere above thunderstorm areas. Comptes Rendus Geoscience, 342, 312-322.
8. Liu, N. et al. (2006). Comparison of results from sprite streamer modeling with spectrophotometric measurements by ISUAL instrument on FORMOSAT-2 satellite. GRL, 33(1), L01101.
9. Liu, N., & Pasko, V. (2004). Effects of photoionization on propagation and branching of positive and negative streamers in sprites. Journal of Geophysical Research (Space Physics), 109(A4), A04301.
10. Janches, D. et al. (2006). Modeling the global micrometeor input function in the upper atmosphere observed by high power and large

aperture radars. Journal of Geophysical Research (Space Physics), 111(A7), A07317.

11. Suszcynsky, D. et al.. (1999). Video and photometric observations of a sprite in coincidence with a meteor-triggered jet event. JGR, 104(D24), 31361-31368.

12. Rubin, A., & Grossman, J. (2010). Meteorite and meteoroid: New comprehensive definitions. MAPS, 45(1), 114-122.

13. Matsudo, Y. et al.. (2009). Comparison of time delays of sprites induced by winter lightning flashes in the Japan Sea with those in the Pacific Ocean. Journal of Atmospheric and Solar-Terrestrial Physics, 71(1), 101-111.

14. Soula, S et al. (2010). Characteristics and conditions of production of transient luminous events observed over a maritime storm. Journal of Geophysical Research (Atmospheres), 115(D16), D16118.

15. Barrington-Leigh, C. P. et al.(1999), Sprites triggered by negative lightning discharges, Geophys. Res. Lett.,26, 3605 – 3608.

16. Tierney, H.E.et al (2005), Radio frequency emissions from a runaway electron avalanche model compared with intense, transient signals from thunderstorms. J. Geophys. Res. 110, D12109, doi:10.1029/2004JD005381

17. Briggs, M. et al. (2013). Terrestrial gamma-ray flashes in the Fermi era: Improved observations and analysis methods. Journal of Geophysical Research (Space Physics), 118(6), 3805-3830.

18. Roberts, O. et al. (2018). The First Fermi-GBM Terrestrial Gamma Ray Flash Catalog. Journal of Geophysical Research (Space Physics), 123(5), 4381-4401.

19. Briggs, M. et al. (2010). First results on terrestrial gamma ray flashes from the Fermi Gamma-ray Burst Monitor. Journal of Geophysical Research (Space Physics), 115(A7), A07323

20. Fishman, G. et al. (1994). Discovery of Intense Gamma-Ray Flashes of Atmospheric Origin. Science, 264(5163), 1313-1316.

21. Yair, Y. et al. (2009). A study of the possibility of sprites in the atmospheres of other planets. Journal of Geophysical Research (Planets), 114(E9), E09002.

22. Giles, R. S. et al. (2020). Possible transient luminous events observed in Jupiter's upper atmosphere. Journal of Geophysical Research: Planets, 125, e2020JE006659.

23. Voss, H. et al. (1998), Satellite observations of lightning induced electron precipitation, J. Geophys. Res., 103, 11,725 – 11,744.

24. Kavanagh, A. et al. (2018). Radiation Belt Slot Region Filling Events: Sustained Energetic Precipitation Into the Mesosphere. Journal of Geophysical Research (Space Physics), 123(9), 7999-8020.

25. Pasko, V. et al.(1998). Ionospheric effects due to electrostatic thundercloud fields. Journal of Atmospheric and Solar-Terrestrial Physics, 60(7-9), 863-870.

26. Lehtinen, et al. (1997). A two-dimensional model of runaway electron beams driven by quasi-electrostatic thundercloud fields. \grl, 24(21), 2639-2642.

27. Saint-Gobain Crystals - Lanthanum Bromide Scintillators Performance Summary. (n.d.). Retrieved July 20, 2022, from https://www.crystals.saint-gobain.com/radiation-detection-scintillators/crystal-scintillators/lanthanum-bromide-labr3

28. https://www.rfa.space/launcher/, 20.07.2022

29. https://www.isaraerospace.com/spectrum, 20.07.2022

30. Blanc +, TARANIS MCP: a joint instrument for accurate monitoring of transient luminous event in the upper atmosphere https://www.researchgate.net/profile/Renaud-Binet/publication/321192621_Taranis_MCP_a_joint_instrument_for_accurate_monitoring_of_transient_luminous_event_in_the_upper_atmosphere/links/5d15d26f92851cf44051926e/Taranis-MCP-a-joint-instrument-for-accurate-monitoring-of-transient-luminous-event-in-the-upper-atmosphere.pdf?origin=publication_detail

31. Østgaard, N., et al. (2019). First 10 months of TGF observations by ASIM. Journal of Geophysical Research: Atmospheres, 2019; 124: 14024– 1t